Available online at www.sciencedirect.com

SCIENCE DIRECT

Magnetic Resonance Imaging 23 (2005) 703–710

MAGNETIC RESONANCE IMAGING

Original contributions

White matter changes in multiple sclerosis: correlation of q-space diffusion MRI and ^{1}H MRS

Yaniv Assaf[a,b,*], Joab Chapman[c,d], Dafna Ben-Bashat[a], Talma Hendler[a,d], Yoram Segev[a], Amos D. Korczyn[d,e], Moshe Graif[a,d], Yoram Cohen[f]

[a]*Functional Brain Imaging Laboratory, Tel Aviv Sourasky Medical Center, Tel Aviv 64329, Israel*
[b]*Department of Neurobiochemistry, Faculty of Life Sciences, Tel Aviv University, Ramat Aviv, Tel Aviv 69978, Israel*
[c]*Department of Neurology, Sheba Medical Center, Ramat Gan 52621, Israel*
[d]*Sackler Faculty of Medicine, Tel Aviv University, Tel Aviv 69978, Israel*
[e]*Department of Neurology, Tel Aviv Sourasky Medical Center, Tel Aviv and the Sieratzki chair of neurology, Tel Aviv University, Tel Aviv 64239, Israel*
[f]*School of Chemistry, The Raymond and Beverly Sackler Faculty of Exact Sciences, Tel Aviv University, Ramat Aviv, Tel Aviv 69978, Israel*

Received 17 January 2005; accepted 22 April 2005

Abstract

Objective: To explore the diagnostic usefulness of high b-value diffusion magnetic resonance brain imaging ("q-space" imaging) in multiple sclerosis (MS). More specifically, we aimed at evaluating the ability of this methodology to identify tissue damage in the so-called normal-appearing white matter (NAWM).

Design: In this study we examined the correlation between q-space diffusion imaging and magnetic resonance spectroscopy (MRS)-based two-dimensional ^{1}H chemical shift imaging. Eight MS patients with different degree of disease severity and seven healthy subjects were scanned in a 1.5-T magnetic resonance imaging (MRI) scanner. The MRI protocol included diffusion tensor imaging (DTI) (with b_{max} of 1000 s/mm^2), high b-value diffusion-weighted imaging (with b_{max} of 14,000 s/mm^2) and 2D chemical shift imaging. The high b-value data set was analyzed using the q-space methodology to produce apparent displacement and probability maps.

Results: We found that the q-space diffusion displacement and probability image intensities correlated well with *N*-acetylaspartate levels ($r = .61$ and .54, respectively). Furthermore, NAWM that was abnormal on MRS was also found to be abnormal using q-space diffusion imaging. In these areas, the q-space displacement values increased from 3.8 ± 0.2 to 4.6 ± 0.6 μm ($P < .02$), the q-space probability values decreased from 7.4 ± 0.3 to 6.8 ± 0.3 ($P < .002$), while DTI revealed only a small, but still significant, reduction in fractional anisotropy values from 0.40 ± 0.02 to 0.37 ± 0.02 ($P < .05$).

Conclusion: High b-value diffusion imaging can detect tissue damage in the NAWM of MS patients. Despite the theoretical limitation of this method, in practice it provides additional information which is clinically relevant for detection of tissue damage not seen in conventional imaging techniques.

Keywords: Multiple sclerosis; MRI; Diffusion MRI; High b value; MRS; NAA

1. Introduction

Multiple sclerosis (MS) is a disease of the central nervous system that involves mainly the white matter (WM) [1,2]. Demyelination is believed to be the main pathological process in MS, although the exact mechanisms leading to it are not well understood [1,2]. Magnetic resonance imaging (MRI) enables detection of lesions in the WM of MS patients, often referred to as MS plaques [3–5]. However, postmortem histological studies have revealed pathological damage in WM areas that appeared normal in conventional MRI [normal-appearing white matter (NAWM)]. This damage consisted of, inter alia astrogliosis, blood–brain barrier breakdown, reduced myelin density and axonal loss [6]. Indeed, in many cases, the disease load as measured by the volume and number of these lesions correlates only poorly with the neurological condition of the patient [4,5].

* Corresponding author. Department of Radiology, The Wohl Institute for Advanced Imaging, Tel Aviv Sourasky Medical Center, Tel Aviv 64239, Israel. Tel.: +972 3 6973039; fax: +972 3 6973080.
E-mail address: assafyan@post.tau.ac.il (Y. Assaf).

0730-725X/$ – see front matter © 2005 Elsevier Inc. All rights reserved.
doi:10.1016/j.mri.2005.04.008

The measurement of *N*-acetylaspartate (NAA) levels using magnetic resonance spectroscopy (MRS) is considered to be the most sensitive method to detect pathology in the NAWM of MS patients [7–10]. *N*-Acetylaspartate is a sensitive neuronal marker [11,12] that can reflect neuronal damage prior to changes in T1- and T2-weighted images. Indeed, it was shown that NAA levels, as detected by MRS, decrease significantly in lesions and also in the NAWM of MS patients [8–10]. However, MRS suffers from low spatial resolution and reproducibility.

High b-value q-space imaging is a recent development of diffusion MRI that was shown to be sensitive toward demyelination and WM changes in animal models [13,14]. The q-space method measures the displacement distribution profile of water molecules in the tissue [13–16]. This profile can be quantified by its width (displacement index) or height (probability index). Using the displacement distribution profile it is possible to distinguish quite accurately between free and restricted modes of diffusion, at sufficiently long diffusion time and high b value [15]. It has been suggested that the axonal content (the neurofilaments) and the myelin layers might restrict water motion although other factors may contribute as well (e.g., restricted diffusion in the extracellular space) [13,14,17]. Therefore, it is assumed that the q-space method emphasizes the contribution of restricted diffusion components in WM, reflecting axonal damage with higher sensitivity.

Recently we have shown that high b-value diffusion data can be used to extract q-space displacement and probability images of the human brain acquired on a clinical scanner [18]. Although clinical human scanners cannot meet the requirements of the q-space theory (i.e., the use of long gradient pulses), the apparent displacement and probability maps were found to be diagnostically beneficial. In areas of MS lesions, a marked increase in the apparent displacement index and a reduction in the apparent probability index were found [18]. These changes most probably result from demyelination and tissue disintegration. Furthermore, significant changes were found both in the apparent displacement and in the probability indices in many areas of NAWM [18]. The pathophysiological mechanisms that underlie the high sensitivity of q-space imaging for detection of WM abnormalities in MS are not understood. Therefore, this work aimed at exploring the metabolic factors that underlie abnormal measures at high b value and thus to validate the findings of the q-space methodology. To this end, we correlated high b-value q-space imaging with NAA/creatinine (Cr) ratios as extracted from ^{1}H two-dimensional chemical shift imaging (2D ^{1}H-CSI).

2. Methods

2.1. Subjects

Magnetic resonance imaging scans were acquired from eight MS patients (see Table 1) and seven normal healthy subjects with no history of neurological disease who served as a control group. The groups were matched for age and gender. The average ages in the MS and control groups were 41±16 and 35±17 years, respectively (nonsignificant difference). The local IRB committee approved the MRI protocol and informed consent was obtained from all participants.

Table 1
Patient list

Patient no.	Age (years)	Sex	Disease duration (years)	Disease type	EDSS
1	43	F	12	RR	2.0
2	33	M	4	SP	6.0
3	21	F	2	RR	0.0
4	28	F	12	SP	4.5
5	75	F	32	SP	6.0
6	48	M	19	RR	2.5
7	40	M	2	RR	3.5
8	46	F	13	RR	3.0

RR, relapsing remitting; SP, secondary progressive.

2.2. Magnetic resonance imaging protocol

Magnetic resonance imaging was performed on a 1.5-T GE Signa horizon echo speed LX MRI scanner (GE, Milwaukee, WI, USA). In all MRI scans the field of view (FOV) was 24 cm, slice thickness was 4.5 mm with 1-mm gaps between slices. The MRI protocol included, in addition to some conventional clinical MR images (T2-weighted MRI, FLAIR and T1-weighted spoiled gradient echo), the high b value (q-space imaging), diffusion tensor imaging (DTI) and chemical shift imaging (CSI) series.

The q-space diffusion data set was acquired using a spin-echo diffusion-weighted echo-planar imaging (DW-EPI) sequence (without cardiac gating) with the following parameters: TR/TE=1500/167 ms, Δ/δ=71/65 ms (where Δ is the diffusion time and δ is the diffusion gradient length), matrix dimension of 128×128 (reconstructed to 256×256) and number of averages=4. The diffusion gradients were applied in six directions [xy, xz, yz, $(-x)y$, $(-x)z$ and $y(-z)$]. The magnitude of the gradients was incremented linearly from 0 to 2.2 G/cm (in 16 steps) to reach a maximal b value of 14,000 s/mm^2 and a maximal q value of 850 cm^{-1}. The q-space data set included 96 images per slice (16 diffusion images×6 diffusion gradient directions), the number of slices was 5 (two at the ventricles and three below it) with total acquisition time of 12 min.

The DTI data set was also acquired using a spin-echo DW-EPI sequence (without cardiac gating) with the following parameters: TR/TE=6000/90 ms, Δ/δ=31/25 ms, g_{max} of 2.2 G/cm (where g_{max} is the maximal value of the diffusion gradient pulse), matrix dimension of 128×128 (interpolated to 256×256), with four averages and 24 slices (five of them being aligned in the same position as the q-space imaging slices). The diffusion images were acquired along the aforementioned diffusion gradient directions with

a maximal b value of 1000 s/mm^2. The DTI data set consisted of seven images (six diffusion images and one with no applied diffusion gradients). The total acquisition time for the DTI data set was 3 min. The 2D ^{1}H-CSI data set was acquired using a PRESS sequence with the following parameters: TR/TE=1600/135 ms, matrix dimension of 16×16, FOV of 20 cm, slice thickness of 12 mm (giving voxel size of ~11×11×12 mm^3) and two averages. The total acquisition time for the CSI was 14 min. The total experimental time for the whole MRI protocol was no longer than 60 min.

2.3. Image and statistical analysis

The q-space analysis of the high b-value DWI data was performed on a pixel-by-pixel basis as previously described [18]. Fractional anisotropy (FA) images were obtained from the DTI data set according to the procedure described by Basser and Pierpaoli [19]. The NAA/Cr ratio was calculated from peak heights for each pixel in the 2D ^{1}H-CSI data set. The line-width of the two peaks was similar and reached approximately 10 Hz. Correlations between NAA/Cr ratios and displacement values were calculated by comparing the mean value of the displacement images in a region of interest (ROI) that corresponded with the CSI voxels. The data set consisted only of pixel that had pure WM without effect of partial volume. To that end the CSI voxel grid was coregistered with FLAIR and T1-weighted spoiled gradient echo images. This way we could omit CSI voxels that had contribution from the cerebrospinal fluid (CSF) of gray matter. Also, we could discriminate between CSI voxels that are in areas of NAWM or in areas of lesions. The CSI data were used to classify the ROI groups according to the following division:

- Group 1 CSI voxels in WM areas of healthy subjects (NAA/Cr values >1.9).
- Group 2 CSI voxels in NAWM areas of MS patients with normal NAA/Cr values (>1.9).
- Group 3 CSI voxels in NAWM areas of MS patients with abnormal NAA/Cr values (<1.9).
- Group 4 CSI voxels in areas of MS plaques (as determined by the FLAIR images).

Mean values of each of the parameters (displacement, probability and FA) were calculated for each group for each patient and than averaged over the whole patient group. The Mann–Whitney *U* test was used to compare q-space displacement, q-space probability and FA values of Group 1 (healthy controls) to each of the three MS groups (see above). Repeated-measures analysis of variance was used to compare the three MS groups. Post hoc comparisons between MS subgroup combinations (Group 2 with Group 3, Group 2 with Group 4, and Group 3 with Group 4) were done using the Scheffe test.

3. Results

Fig. 1 shows FLAIR, FA, q-space displacement and probability images for a healthy volunteer and two MS patients. The FLAIR images of the MS patients show several hyperintense areas that were denoted as MS lesions (Fig. 1E and I). The FA images show significant reduction in the image intensity in the areas of MS lesions (see arrows

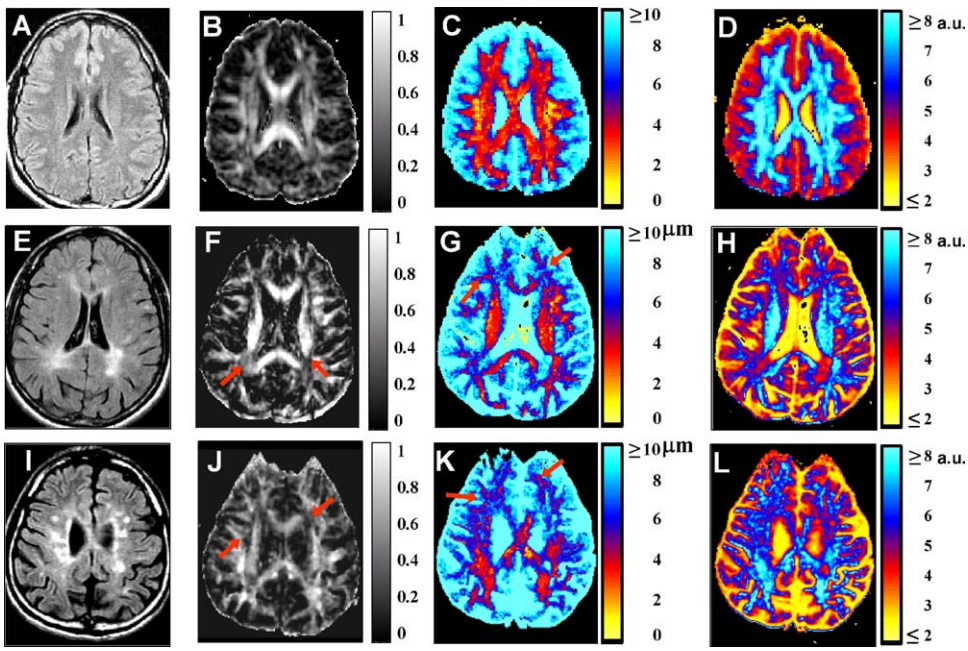

Fig. 1. MRI data of a healthy subject and two MS patients including FLAIR (left column), FA (second column), q-space displacement images (third column) and q-space probability images (fourth column). The healthy subject (images A–D) had no history of neurological disorders. The first MS patient (images E–H) had extended disability severity score (EDSS) of 3.5 (Patient 7 in Table 1) while the second patient (images I–L) had an EDSS of 6.0 (Patient 2 in Table 1). Arrows indicate areas of abnormal image intensity in MS lesions (FA images F and J) and in NAWM (displacement imaging G and K).

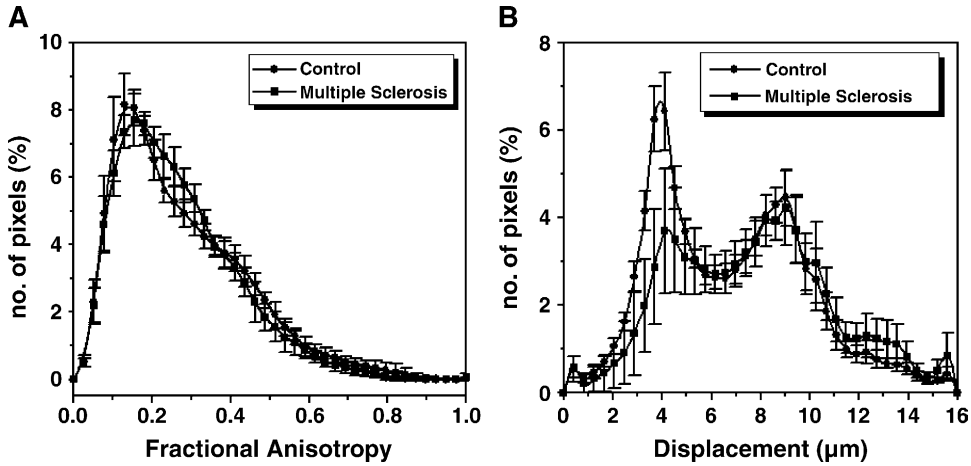

Fig. 2. Histograms of the FA images (A) and q-space displacement (B) images averaged over all subjects and patients scanned in this study. Circles represent data of the control group ($n=7$) and the squares represent data of the MS group ($n=8$).

in Fig. 1F and J). The q-space displacement images show marked reduction in the displacement values in areas of hyperintensity in the FLAIR images (MS lesions) (Fig. 1G and K). In the same areas, the q-space probability images (Fig. 1H and L) show significant reduction in the probability values. In addition, it is possible to detect abnormal intensity in the displacement and probability images in large areas of the NAWM (see arrows in Fig. 1G and K) as compared to healthy subjects (see red-yellow areas in Fig. 1C). However, it is very difficult to detect these changes in the FA images (Fig. 1F and J). Fig. 2 shows histograms of the FA values and q-space displacement values averaged separately for controls and patients (Fig. 2A and B, respectively). Histograms were generated from the whole acquired brain volume. The histograms of the FA values, obtained from conventional DTI, show only minor differences between the MS and control groups (Fig. 2A). It seems that there is a small increase in the number of pixels with low anisotropy (FA values of 0.2–0.3) and a small decrease in the number of pixels with high anisotropy (FA values of 0.6 and higher). However, the histograms of the q-space displacement values of the two groups show much larger differences (Fig. 2B). The displacement value histogram for the control group shows three peaks that correspond to WM (displacement range, 1–4 μm), gray matter (5–9 μm) and CSF (10–14 μm). The WM peak is significantly reduced in the displacement histograms of the MS group as compared with the control group ($P<.001$). On the other hand, the peak in the range between 10 and 14 μm (which was attributed to CSF in the control group) seems to be larger for the MS group as compared with the control group (Fig. 2B) ($P<.03$).

Fig. 3 shows the classification into ROI groups according to the 2D ^{1}H-CSI data. Fig. 3A portraits the FLAIR image

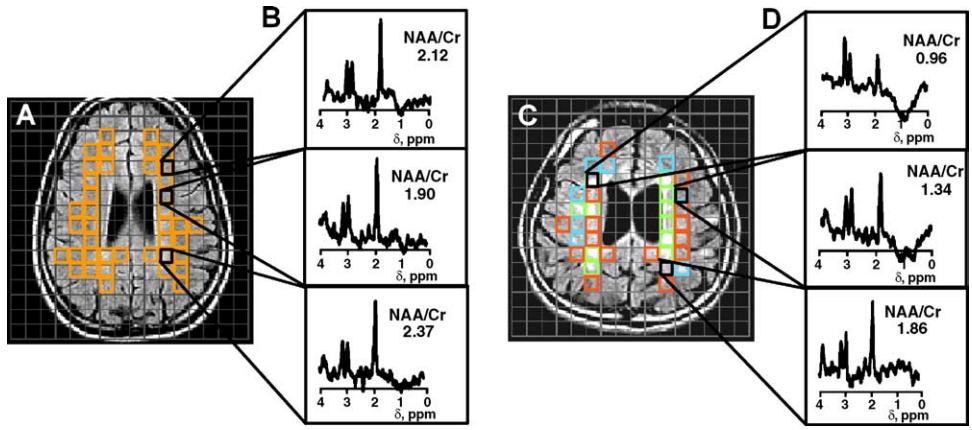

Fig. 3. Classification of ROI based on CSI data. (A) FLAIR image of a healthy subject on which the CSI gridlines are superimposed. The transparent white squares represent areas of WM that were referred to as Group 1. (B) MR spectra taken from three ROIs of Group 1 showing normal distribution of NAA/Cr ratios. (C) FLAIR image of an MS patient (Patient 2 in Table 1) on which the CSI gridlines are superimposed. The red squares represent areas of NAWM that have normal NAA/Cr ratio (Group 2). The blue squares represent areas of NAWM that have abnormal NAA/Cr ratio (Group 3). The 19 green squares represent areas of WM that contain MS lesions (as detected by FLAIR); these areas were considered as Group 4. (D) MR spectra taken from three ROIs shown in C that represent ROI of Group 4 (top spectrum), Group 3 (middle spectrum) and Group 2 (bottom spectrum).

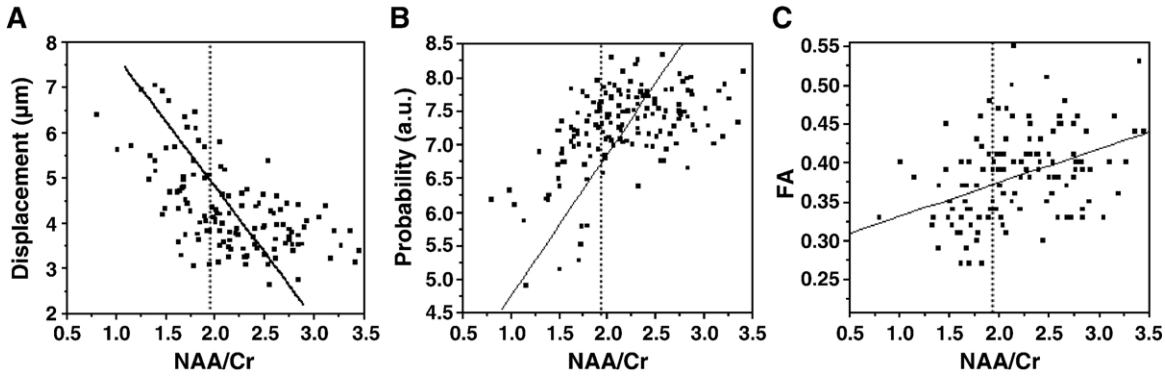

Fig. 4. (A) Correlation between q-space displacement values and NAA/Cr ratio ($r=-.61$, $P<.001$). (B) Correlation between q-space probability values and NAA/Cr ratio ($r=.53$, $P<.001$). (C) Correlation between FA values and NAA/Cr ratio ($r=.43$, $P<.003$). Each point represents data collected from a CSI voxel. The data shown in this figure were collected from all subjects. The dotted lines represent the NAA/Cr value of 1.9, in which above it areas were treated as normal and below it as abnormal WM.

of a control subject on which the grid lines of the CSI were superimposed. The orange squares in this image represent ROIs in the WM that were classified as normal WM (Group 1). Fig. 3B shows three spectra taken from three CSI voxels of this healthy subject. Fig. 3C shows a FLAIR image of an MS patient on which the grid lines of the CSI were superimposed. The green squares represent ROIs in areas of MS lesions (Group 2). The blue squares represent ROIs in areas of NAWM that have an abnormal NAA/Cr ratio (lower than 1.8) (Group 3). The red squares represent ROIs in areas of NAWM that were found to have normal NAA/Cr values (Group 4).

Fig. 4 shows scatterplots of correlation analyses between the NAA/Cr values and the corresponding q-space displacement, probability and FA values (Fig. 4A–C, respectively). The correlation between NAA/Cr values and the q-space displacement values (Fig. 4A) and probability values (Fig. 4B) for all ROI groups as described in Fig. 3 is significant ($r=-.61$, $P<.001$ and $r=.53$, $P<.001$, respectively). Fig. 4C demonstrates the correlation between NAA/Cr values and the FA values. This correlation was found to be less significant ($r=.43$, $P<.003$) than the correlation with the displacement values. Fig. 5 shows the q-space displacement, probability and FA values of the different ROI groups as defined in Fig. 3. Fig. 5A shows a box graph for the mean displacement values of the different groups. The mean displacement value of Group 1 (WM of healthy subjects) was 3.9 ± 0.2 μm. The mean displacement value for Group 2 (normal NAA/Cr values in MS patients) was found to be similar to that of Group 1 (3.7 ± 0.2 μm). The mean displacement value for Group 3 (abnormal NAA/Cr values in MS patients) was 4.6 ± 0.6 μm (a 24% increase compared to Group 2). This value is statistically different from both the values of Groups 1 and 2 ($P<.02$ in both cases). The mean displacement value in MS lesions (Group 4) was found to be 6.9 ± 0.6 (an 86% increase compared to Group 2) and statistically different from the values of all other groups ($P<.001$ for all groups). Fig. 5B shows a box graph for the q-space probability values of the different groups. The mean probability value of Group 2 was 7.4 ± 0.3 in arbitrary units (a.u.) similar to that of Group 1 (7.5 ± 0.4 a.u.). The mean probability of Group 3 was 6.8 ± 0.3, which is statistically different from both Groups 1 and 2 ($P<.002$). The mean probability of Group 4 was

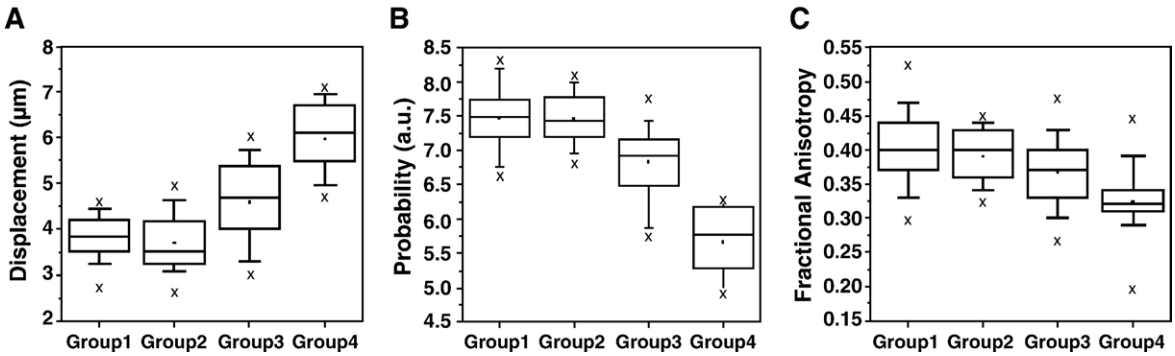

Fig. 5. Box graphs of the displacement values (A), probability values (B) and FA values (C) for each of the four groups described in Fig. 3. The x symbols above and below the box represent maximum and minimum values. Mean values for each group within each patient were first calculated and these values were used to calculate the mean and S.D. (error bars) over the whole patient group. The dot inside each box represents the mean value and the bar inside each box represent the median value.

5.6±0.6, statistically different from all other groups ($P<.001$). Fig. 5C shows a box graph for the FA values for the different ROI groups. The mean FA value of Group 1 (WM of healthy subjects) was 0.40±0.03. The mean FA value for Group 2 (normal NAA/Cr values in MS patients) was similar to that of Group 1 (0.40±0.02). The mean FA value for Group 3 (abnormal NAA/Cr values in MS patients) was 0.37±0.02 (7.5% decrease compared to Group 2). This FA value is not statistically different from Groups 1 and 2. The mean FA value in MS lesions (Group 4) was 0.31±0.05 (a 22.5% decrease from Group 2) and statistically different from all groups ($P<.001$ for all groups).

4. Discussion

Magnetic resonance imaging is an important imaging modality for the diagnosis and follow-up of MS. Therefore, most of the pharmacological effects of therapeutic interventions in MS are evaluated using MRI. In the majority of the MRI studies, the disease load in the brain is estimated by the volume and number of MS lesions detected by T2 or FLAIR images despite the accepted view that tissue damage in MS exceeds the areas of MS lesions observed in conventional MRI studies using T2 and FLAIR. Although MRS can detect abnormal metabolite concentration in areas of NAWM, usually as reduced NAA/Cr ratio, the clinical use of this method is limited mainly due to low spatial resolution.

4.1. Diffusion tensor imaging in MS

Among the advanced WM-specific imaging techniques, DTI seems to provide the best gray matter/WM contrast. Diffusion tensor imaging enables differentiation between gray matter and WM based on the different diffusion properties of those tissues [19,20]. In gray matter, the diffusion of water molecules is mostly isotropic, that is, similar in any measured direction. By contrast, in the WM the diffusion is anisotropic due to hindered and restricted diffusion perpendicular to the long axis of the neuronal fibers [19,20]. Since DTI is more sensitive to WM than other imaging techniques, it was assumed that the FA index, extracted from DTI, would show subtle damage in the NAWM of MS patients. In fact, there was a small reduction in the FA in NAWM areas as compared to healthy volunteers [18,21–23]. This point is emphasized in the FA histogram demonstrated in Fig. 2A, which shows a very small reduction in the FA values of MS patients, observed mainly in the high anisotropy range (0.5–0.8). The relation between the FA of the water signal in WM and myelin content (believed to be damaged in MS) is questionable, and several studies point to the fact that diffusion anisotropy (measured at low b values) may be observed even in the absence of myelin [24,25]. Diffusion tensor imaging is believed to measure mainly the diffusion anisotropy of water molecules in the extracellular space [26]. Indeed, the diffusion in extracellular space between aligned neuronal fibers is most probably anisotropic enough to produce good gray matter to WM contrast. However, it might not be sensitive enough for detection of myelin disruption or intra-axonal damage when less extensive as in the NAWM of MS patients. However, in MS lesions, where the structural damage is more pronounced, the FA index shows greater differences.

4.2. High b-value q-space imaging in MS

In contrast to low b-value DTI, the signal intensity in high b-value DWI was found to depend on restricted diffusion [13,17]. It was suggested that one of the main components of restricted water motion in neuronal tissue is that of intra-axonal water when the diffusion is measured perpendicular to the fibers. The q-space analysis was suggested as a tool for quantification of restricted diffusion in neuronal tissue emphasizing the contribution of this component [13,17]. Although the q-space methodology was theoretically developed for experimental conditions that cannot be met in clinical scanners, it was found that performing these experiments under experimental "clinical" conditions is diagnostically beneficial [18]. Indeed, the extracted q-space parameters (displacement and probability) should be better termed *apparent displacement and apparent probability*. Nevertheless, the low gradient amplitude produced by human scanners requires the use of long gradient pulse durations (δ), long diffusion time periods (Δ) and hence long echo time in order to achieve high b values sufficient for characterization of the slow diffusion component. However, by using these unfavorable experimental conditions, the restricted component is overemphasized and its relative contribution is artificially exaggerated [18]. Therefore, any damage to the axonal milieu may lead to reduction in the restricted diffusion that can be probed with relatively high sensitivity using the q-space method.

The histogram in Fig. 2B shows the ability of the q-space method to discriminate between the different diffusing components in the brain (WM, gray matter and CSF) based on their mean displacement during the diffusion time as measured at high b values. Water molecules are restricted when measured perpendicular to the axons; thus, the displacement there is much less than in gray matter and CSF, producing a separate peak for WM in the displacement histograms (Fig. 2B). This peak is significantly reduced in the MS images as compared with the control group. This may be a result of a decrease in the restricted diffusion in some areas of the WM in MS. Indeed, the q-space images reveal large abnormal areas, exceeding the regions of the apparent MS lesions, suggesting a more diffuse nature of the disease (Fig. 1).

4.3. Correlation with CSI findings

The q-space method reveals tissue abnormalities that exceed the area of obvious MS lesions, reflecting the high sensitivity of this method. Although this sensitivity can be

related to changes in the extent of restricted diffusion of water molecules, this can only be verified by histology. Studies on animal models showed good correlation between histological findings and q-space imaging measurements [14,27]. One in vivo parameter that can be used for validation of q-space imaging findings is NAA levels as detected by MRS. The NAA/Cr ratios were shown to be a sensitive parameter for detection of abnormal WM tissue in the NAWM of MS patients [8–10]. The major observation of MRS studies in MS is reduced NAA levels in wide areas of the NAWM suggestive of axonal loss [8–10]. Therefore, correlating between spectroscopic findings and q-space imaging may provide the needed validation of the q-space method in MS. Indeed, a good correlation was found between the two indices (NAA/Cr ratio and q-space displacement or probability) (r=.61 and .53; Fig. 4A and B).

In this study we used NAA/Cr values to classify ROIs in MS into groups (healthy NAWM and abnormal NAWM; see Fig. 3). Region of interest analysis of q-space displacement and FA images was performed using this classification. Displacement and probability values in abnormal NAWM were found to be statistically different from those of "healthy" NAWM in MS patients (Fig. 5A and B). However, the FA values of these two groups (Groups 2 and 3) were not statistically different (Fig. 5C). These results reflect the greater sensitivity of q-space imaging as compared with FA toward tissue damage in the WM, which is undetected by routine MR imaging. In MS lesions, q-space imaging reports of 86% increase in the displacement values (with 13% relative S.D.) compared with only 23% decrease in FA (with 16% relative S.D.). The high sensitivity is even more impressive in the areas of the NAWM where only subtle WM damage occurs. In these areas there was an increase of 23% in the displacement value (with relative S.D. of 14%) compared with only 7.5% decrease in the FA (with a relative S.D. of 13%). The ability of q-space imaging to demonstrate on differences in displacement values, 1.5 times higher than the S.D., by using this methodology, suggests that it may be possible to detect WM damage in the NAWM for a single patient. It seems that the q-space diffusion MRI may have an impact on the management of MS patients as it measures larger areas of tissue damage that may reflect the real pathological condition of the brain tissue. This may help in better evaluation of the therapeutic performance of new and known drugs for treatment of MS and other WM disorders.

Acknowledgments

The authors thank the Adams Super Center For Brain Studies (Tel Aviv University) for financial support. Support of this project by the German Federal Ministry of Education and Research within the framework of the German-Israeli Projects Cooperation (DIP) (to Y.C.) is also gratefully acknowledged. The Ministry of Science and Technology is acknowledged for financial support (to Y.A.). We also thank the Adams Super Center for Brain Studies of Tel Aviv University for financial support (to Y.C. and Y.A.). We wish to thank Mr. Tom Schonberg for help with statistical analysis. In addition, we thank all the patients and volunteers who participated in this study.

References

[1] McFarlin DE, McFarland HF. Multiple sclerosis. N Engl J Med 1982; 307:1183–8.
[2] Compston A, Ebers G, Lassmann H. McAlpine's multiple sclerosis. Cambridge: Churchill Livingstone; 1997.
[3] Fazekas F, Barkhof F, Filippi M, et al. The contribution of magnetic resonance imaging to the diagnosis of multiple sclerosis. Neurology 1999;53:448–56.
[4] Barkhof F, van Walderveen M. Characterization of tissue damage in multiple sclerosis by nuclear magnetic resonance. Philos Trans R Soc Lond B 1999;354:1675–86.
[5] Barkhof F. The clinico-radiological paradox in multiple sclerosis revisited. Curr Opin Neurol 2002;15:239–45.
[6] Allen IV, McQuaid S, Mirakhur M, Nevin G. Pathological abnormalities in the normal-appearing white matter in multiple sclerosis. Neurol Sci 2001;22:141–4.
[7] Filippi M, Tortorella C, Bozzali M. Normal-appearing white matter changes in multiple sclerosis: the contribution of magnetic resonance techniques. Mult Scler 1999;5:273–82.
[8] Rooney WD, Goodkin DE, Schuff N, et al. H-1 MRSI of normal appearing white matter in multiple sclerosis. Mult Scler 1997;3:231–7.
[9] Leary SM, Davie CA, Parker GJM, et al. H-1 Magnetic resonance spectroscopy of normal-appearing white matter in primary progressive multiple sclerosis. J Neurol 1999;246:1023–6.
[10] Cucurella MG, Rovira A, Rio J, et al. Proton magnetic resonance spectroscopy in primary and secondary progressive multiple sclerosis. NMR Biomed 2000;13:57–63.
[11] van der Knaap MS, van der Grond J, Luyten PR, et al. H-1 and 31-P magnetic-resonance spectroscopy of the brain in degenerative cerebral-disorders. Ann Neurol 1992;31:202–11.
[12] Tsai GC, Coyle JT. *N*-acetylaspartate in neuropsychiatric disorders. Prog Neurobiol 1995;46:531–40.
[13] Assaf Y, Mayk A, Cohen Y. Displacement imaging of spinal cord using q-space diffusion-weighted MRI. Magn Reson Med 2000;44: 713–22.
[14] Cohen Y, Assaf Y. High *b* value q-space analyzed diffusion-weighted MRS and MRI in neuronal tissues. NMR Biomed 2002;15:516–42.
[15] Cory DG, Garroway AN. Measurement of translational displacement probabilities by NMR: an indicator of compartmentation. Magn Reson Med 1990;14:435–44.
[16] Callaghan PT, Coy A, MacGowan D, Packer KJ, Zelaya FO. Diffraction-like effects in NMR diffusion studies of fluids in porous solids. Nature 1991;351:467–9.
[17] Assaf Y, Cohen Y. Assignment of the water slow diffusing component in CNS using q-space diffusion MRS: implications for fiber tract imaging. Magn Reson Med 2000;43:191–9.
[18] Assaf Y, Ben-Bashat D, Chapman J, et al. High *b*-value *q*-space analyzed diffusion-weighted MRI: application to multiple sclerosis. Magn Reson Med 2002;47:115–26.
[19] Basser PJ, Pierpaoli C. A simplified method to measure diffusion tensor from seven MR images. Magn Reson Med 1998;39:928–34.
[20] Basser PJ, Mattiello J, Le-Bihan D. Estimation of the effective self-diffusion tensor from the NMR spin echo. J Magn Reson B 1994;103: 247–54.
[21] Guo AC, MacFall JR, Provenzale JM. Multiple sclerosis: diffusion tensor MR imaging for eventuation of normal appearing white matter. Radiology 2002;222:729–36.

[22] Werring DJ, Clark CA, Barker GD, et al. Diffusion tensor imaging of lesions and normal-appearing white matter in multiple sclerosis. Neurology 1999;52:1626–32.

[23] Bammer R, Augustin M, Strasser-Fuchs S, et al. Magnetic resonance diffusion tensor imaging for characterizing diffusion and focal white matter abnormalities in multiple sclerosis. Magn Reson Med 2000;44: 583–91.

[24] Beaulieu C, Fenrich FR, Allen PS. Multicomponent water proton transverse relaxation and T_2-discriminated water diffusion in myelinated and non-myelinated nerve. Magn Reson Imaging 1998;16:1201–10.

[25] Ono J, Harada K, Takahashi M, et al. Differentiation between dysmyelination and demyelination using magnetic resonance diffusional anisotropy. Brain Res 1995;671:141–8.

[26] Kraemer F, Darquie A, Clark CA, Le Bihan D. Separation of two diffusion compartments in the human brain. Proc Int Soc Magn Reson Med 1999;7:1808.

[27] Assaf Y, Kafri M, Shinar H, et al. Changes in axonal morphology in experimental allergic neuritis as studied by q-space ^1H and ^2H DQF diffusion magnetic resonance spectroscopy. Magn Reson Med 2002; 48:71–81.